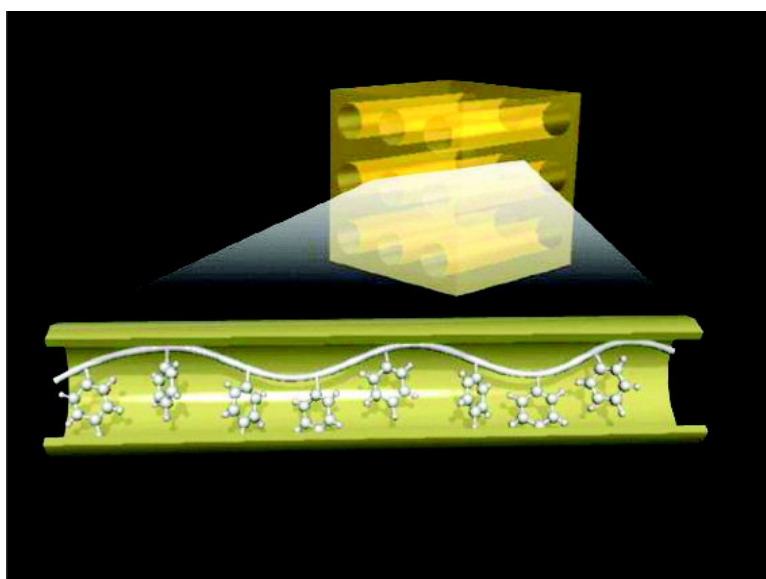


## Conformation and Molecular Dynamics of Single Polystyrene Chain Confined in Coordination Nanospace

Takashi Uemura, Satoshi Horike, Kana Kitagawa, Motohiro Mizuno, Kazunaka Endo, Silvia Bracco, Angiolina Comotti, Piero Sozzani, Masataka Nagaoka, and Susumu Kitagawa

*J. Am. Chem. Soc.*, **2008**, 130 (21), 6781-6788 • DOI: 10.1021/ja800087s • Publication Date (Web): 07 May 2008

Downloaded from <http://pubs.acs.org> on February 8, 2009



### More About This Article

Additional resources and features associated with this article are available within the HTML version:

- Supporting Information
- Access to high resolution figures
- Links to articles and content related to this article
- Copyright permission to reproduce figures and/or text from this article

[View the Full Text HTML](#)



**ACS Publications**  
High quality. High impact.

## Conformation and Molecular Dynamics of Single Polystyrene Chain Confined in Coordination Nanospace

Takashi Uemura,<sup>†,‡</sup> Satoshi Horike,<sup>†</sup> Kana Kitagawa,<sup>†</sup> Motohiro Mizuno,<sup>§</sup>  
Kazunaka Endo,<sup>§</sup> Silvia Bracco,<sup>||</sup> Angiolina Comotti,<sup>||</sup> Piero Sozzani,<sup>||</sup>  
Masataka Nagaoka,<sup>⊥,#</sup> and Susumu Kitagawa<sup>\*,†,+</sup>

Department of Synthetic Chemistry and Biological Chemistry, Graduate School of Engineering, Kyoto University, Katsura, Nishikyo-ku, Kyoto 615-8510, Japan, PRESTO, Japan Science and Technology Agency (JST), Honcho Kawaguchi, Saitama 332-0012, Japan, Department of Chemistry, Graduate School of Natural Science and Technology, Kanazawa University, Kanazawa 920-1192, Japan, Department of Materials Science, University of Milano-Bicocca, via R. Cozzi 53, 20125 Milan, Italy, Department of Complex Systems Science, Graduate School of Information Science, Nagoya University, Furo-chou, Chikusa-ku, Nagoya 464-8601, Japan, and CREST, JST, Japan, and Institute for Integrated Cell-Material Sciences (iCeMS), Kyoto University, Yoshida, Sakyo-ku, Kyoto 606-8501, Japan

Received January 5, 2008; E-mail: kitagawa@sbchem.kyoto-u.ac.jp

**Abstract:** Molecules confined in nanospaces will have distinctly different properties to those in the bulk state because of the formation of specific molecular assemblies and conformations. We studied the chain conformation and dynamics of single polystyrene (PSt) chains confined in highly regular one-dimensional nanochannels of a porous coordination polymer  $[Zn_2(bdc)_2ted]_n$  (1; bdc = 1,4-benzenedicarboxylate, ted = triethylenediamine). Characterization by two-dimensional (2D) heteronuclear  $^1H$ - $^{13}C$  NMR gave a direct demonstration of the nanocomposite formation and the intimacy between the PSt and the pore surfaces of 1. Calorimetric analysis of the composite did not reveal any glass transition of PSt, which illustrates the different nature of the PSt encapsulated in the nanochannels compared with that of bulk PSt. From  $N_2$  adsorption measurements, the apparent density of PSt in the nanochannel was estimated to be  $0.55 \text{ g cm}^{-3}$ , which is much lower than that of bulk PSt. Results of a solid-state  $^2H$  NMR study of the composite showed the homogeneous mobility of phenyl flipping with significantly low activation energy, as a result of the encapsulation of single PSt chains in one-dimensional regular crystalline nanochannels. This is also supported by molecular dynamics (MD) simulations.

### Introduction

Recently, porous coordination polymers (PCPs) composed of transition metal ions and bridging organic ligands have been extensively studied.<sup>1</sup> The characteristic features of PCPs are highly regular channel structures, controllable channel sizes approximating molecular dimensions, and designable surface potentials and functionality. These features differ from those of conventional porous materials, such as zeolites, activated carbons, and organic supramolecular hosts. Owing to these

advantages, successful applications of PCPs range from molecular storage/separation to heterogeneous catalysts.<sup>1</sup> In particular, there is a considerable interest in studying the confinement effects of molecules accommodated in such specific nanochannels of PCPs.<sup>2</sup> The confined guest molecules show unique properties with regard to molecular motion,<sup>2b,d</sup> phase transition,<sup>2c</sup> charge transfer,<sup>2a,e</sup> and magnetic properties,<sup>2f,g</sup> which are characteristic of low dimensional and nanosized assemblies formed in the specific nanospaces of PCPs. However, in spite of the many reports on small guest molecule systems, studies on confinement effects of macromolecules in the nanospaces of PCPs have not yet been explored, because of a

<sup>†</sup> Department of Synthetic Chemistry and Biological Chemistry, Kyoto University.

<sup>‡</sup> PRESTO, JST.

<sup>§</sup> Kanazawa University.

<sup>||</sup> University of Milano-Bicocca.

<sup>⊥</sup> Nagoya University.

<sup>#</sup> CREST, JST.

<sup>+</sup> iCeMS, Kyoto University.

- (1) (a) Yaghi, O. M.; O'Keeffe, M.; Ockwig, N. W.; Chae, H. K.; Eddaoudi, M.; Kim, J. *Nature* **2003**, *423*, 705. (b) Férey, G.; Mellot-Drazniewski, C.; Serre, C.; Millange, F. *Acc. Chem. Res.* **2005**, *38*, 217. (c) Kitagawa, S.; Kitaura, R.; Noro, S. *Angew. Chem., Int. Ed.* **2004**, *43*, 2334. (d) Bradshaw, D.; Claridge, J. B.; Cussen, E. J.; Prior, T. J.; Rosseinsky, M. J. *Acc. Chem. Res.* **2005**, *36*, 273. (e) Moulton, B.; Zaworotko, M. J. *Chem. Rev.* **2001**, *101*, 1629. (f) Janiak, C. *Dalton Trans.* **2003**, 2781. (g) Kesanli, B.; Lin, W. B. *Coord. Chem. Rev.* **2003**, *246*, 305. (h) Kepert, C. J. *Chem. Commun.* **2006**, 695.

- (2) (a) Choi, H. J.; Suh, M. P. *J. Am. Chem. Soc.* **2004**, *126*, 15844. (b) Horike, S.; Matsuda, R.; Kitaura, R.; Kitagawa, S.; Iijima, T.; Endo, K.; Kubota, Y.; Takata, M. *Chem. Commun.* **2004**, 2152. (c) Ueda, T.; Kurokawa, K.; Omichi, H.; Miyakubo, K.; Eguchi, T. *Chem. Phys. Lett.* **2007**, *443*, 293. (d) Soldatov, D. V.; Moudrakovski, I. L.; Ratcliffe, C. I.; Dutrisac, R.; Ripmeester, J. A. *Chem. Mater.* **2003**, *15*, 4810. (e) Shimomura, S.; Matsuda, R.; Tsujino, T.; Kawamura, T.; Kitagawa, S. *J. Am. Chem. Soc.* **2006**, *128*, 16416. (f) Kitaura, R.; Kitagawa, S.; Kubota, Y.; Kobayashi, T.; Kindo, K.; Mita, Y.; Matsuo, A.; Kobayashi, M.; Chang, H.-C.; Ozawa, T.; Suzuki, M.; Sakata, M.; Takata, M. *Science* **2002**, *298*, 2358. (g) Takamizawa, S.; Nakata, E.; Akatsuka, T. *Angew. Chem., Int. Ed.* **2006**, *45*, 2216.

lack of synthetic methodology as well as the unavailability of suitable analytical methods.

Confined polymers at the nanometer scale exhibit fascinating and unexpected properties, which has led to the emergence of an important new area of research.<sup>3</sup> A variety of thermal, spectroscopic, and theoretical investigations demonstrates them to have unusual polymer conformations and dynamics as well as unique electronic properties.<sup>4</sup> In particular, polymer inclusion in crystalline microporous hosts (pore size < 2 nm) with ordered and well-defined nanochannel structures is attracting much attention. This is largely because this approach can prevent the entanglement of polymer chains and provide extended chains in restricted spaces, in contrast to amorphous bulk polymer systems and polymers in solution.<sup>5</sup> The host–guest systems based on crystalline microporous compounds and organic polymers can be realized by (1) direct self-assembly of host compounds and polymers or (2) polymerization of the monomers accommodated in the host nanochannels. In this field, microporous organic hosts such as ureas, perhydrotriphenylene, cyclotriphosphazenes, cholic acids, and cyclodextrins play dominant roles.<sup>5</sup> However, these organic hosts exploit only hydrogen bonding or weak van der Waals interactions and generally produce narrow channels (ca. 4–6 Å) that often prevent the incorporation of polymer chains with bulky side chains, such as polystyrene (PSt), polyacrylates, and polymethacrylates.

Recently, we have reported on synthetic approaches for inclusion polymerizations of vinyl monomers adsorbed in nanochannels of PCPs and showed nanospace effects on the polymerization, such as monomer reactivity, molecular weight, and the structure of the resulting polymers.<sup>6</sup> Besides the aspect of polymer synthesis, rigid and relatively large open-channel structures of PCPs enable the accommodation of bulky vinyl

polymers in the coordination frameworks, which will create an unusual supramolecular environment for both the confined polymer and the coordination framework. In order to elucidate the physical properties of the polymers in such restricted spaces, studies of the molecular conformation and dynamics are very important, not only for understanding fundamental conformation–property relationships but also, from a practical point of view, for the rational design of polymer-based materials with specific properties.<sup>7</sup> Hence, the regulated and tailor-made pore characteristics of PCPs are of key importance for achieving unique polymer encapsulation systems. We are now able to precisely control the following features within the designable nanochannels of PCPs: (1) the number of polymer chains, (2) the environments for polymers, and (3) the chain orientations. This will contribute to the quantitative analysis of the confined polymer properties and to the preparation of a new class of materials based on PCP–polymer hybridization.

Here, we studied the conformation and molecular dynamics of PSt chains confined in nanochannels ( $7.5 \times 7.5 \text{ \AA}^2$ ) of  $[\text{Zn}_2(\text{bdc})_2\text{ted}]_n$  (**1**; bdc = 1,4-benzenedicarboxylate, ted = triethylenediamine).<sup>6a,d</sup> The advantageous porous character of **1** is a highly regulated one-dimensional nanochannel structure with a smooth and flat surface potential. Thus, only a single PSt chain will be accommodated in the channels of **1** as a linearly extended conformation, based on the molecular dimensions of styrene (St) ( $6.8 \times 4.4 \times 3.3 \text{ \AA}^3$ ). The existence of a large interface between an organic polymer and a metal–organic host was studied, for the first time, by using advanced  $2\text{D } ^1\text{H}-^{13}\text{C}$  solid-state NMR techniques, particularly heteronuclear chemical shift NMR correlation experiments, which highlight neighboring species separated by ca. 1 nm through their dipole–dipole couplings. Using  $^2\text{H}$  NMR measurements that are sensitive to segmental chain motion, we also demonstrated how a linearly extended single PSt chain behaves in the specific nanosized space based on **1**. The chain conformations of PSt oligomers simulated using the molecular dynamics (MD) method supported the unique molecular motion of PSt confined in the nanochannels.

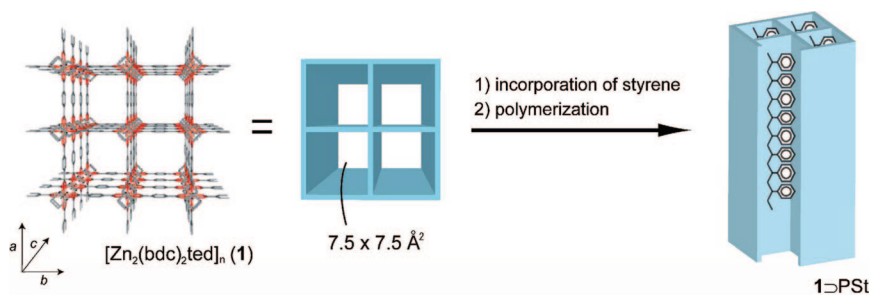
## Experimental Section

**Materials.** All reagents and chemicals were obtained from commercial sources. The styrene monomer (St) was purified by vacuum distillation prior to use. A nanocomposite of PSt with  $[\text{Zn}_2(\text{bdc})_2\text{ted}]_n$  (**1**⊃PSt) was prepared by a previously reported method using the radical polymerization of St adsorbed in the channels of **1**.<sup>6a,d</sup> X-ray powder diffraction (XRPD) measurements of the pure host **1** and **1**⊃PSt showed that the framework structure of **1** was preserved during the polymerization process. The incorporation ratio of PSt in **1** (weight of PSt/ weight of the host **1**) was 0.23, as determined by thermogravimetric analysis (TG). Gel permeation chromatography measurement (GPC) of the polymer after extraction from the nanochannels of **1** showed a molecular weight ( $M_n$ ) of 56 000. The stereoregularity of the PSt included in **1** was similar to that of a bulk PSt sample prepared by conventional radical polymerization, as determined by  $^{13}\text{C}$  NMR measurements (the syndiotacticity of PSt in **1** and bulk PSt were 62% and 63%, respectively).

**Solid-State  $^1\text{H}$  and  $^{13}\text{C}$  NMR.** The solid-state  $^{13}\text{C}$  NMR spectra were run at 75.5 MHz on a Bruker Avance 300 instrument. The

- (3) (a) Sozzani, P.; Bracco, S.; Comotti, A.; Simonutti, R. *Adv. Polym. Sci.* **2005**, *181*, 153. (b) Harada, A.; Li, J.; Kamachi, L. *Nature* **1992**, *356*, 325. (c) Tajima, K.; Aida, T. *Chem. Commun.* **2000**, 2399. (d) Sozzani, P.; Bracco, S.; Comotti, A.; Simonutti, R.; Valsesia, P.; Sakamoto, Y.; Terasaki, O. *Nat. Mater.* **2006**, *5*, 545. (e) Lu, J.; Mirau, P. A.; Tonelli, A. E. *Prog. Polym. Sci.* **2002**, *27*, 357. (f) Pinnavaia, T. J.; Beall, G. W. *Polymer - Clay Nanocomposites*; John Wiley & Sons: New York, 2000.
- (4) (a) Wu, C.-G.; Bein, T. *Science* **1994**, *266*, 1013. (b) Moller, K.; Bein, T. *Chem. Mater.* **1998**, *10*, 2950. (c) Lu, Y.; Yang, Y.; Sellinger, A.; Lu, M.; Huang, J.; Fan, H.; Haddad, R.; Lopez, G.; Burns, A. R.; Sasaki, D. Y.; Shelnut, J.; Brinker, J. *Nature* **2001**, *410*, 885. (d) Cardin, D. J. *Adv. Mater.* **2002**, *14*, 553. (e) Lin, V. S.-Y.; Radu, D. R.; Han, M.-K.; Deng, W.; Kuroki, S.; Shanks, B. H.; Pruski, M. *J. Am. Chem. Soc.* **2002**, *124*, 9040. (f) Smith, R. C.; Fischer, W. M.; Gin, D. L. *J. Am. Chem. Soc.* **1997**, *119*, 4092. (g) Molenkamp, W. C.; Watanabe, M.; Miyata, H.; Tolbert, S. H. *J. Am. Chem. Soc.* **2004**, *126*, 4476. (h) Pattantyus-Abraham, A. G.; Wolf, M. O. *Chem. Mater.* **2004**, *16*, 2180. (i) Sozzani, P.; Comotti, A.; Bracco, S.; Simonutti, R. *Angew. Chem., Int. Ed.* **2004**, *43*, 2792.
- (5) (a) Hollinsworth, M.; Harris, K. D. M. In *Comprehensive Supramolecular Chemistry, Vol. 10*; Pergamon: Oxford, 1996; p 177. (b) Farina, M.; Di Silvestro, G.; Sozzani, P. In *Comprehensive Supramolecular Chemistry, Vol. 10*; Pergamon: Oxford, 1996; p 371. (c) Schilling, F. C.; Amduson, K. R.; Sozzani, P. *Macromolecules* **1994**, *27*, 6498. (d) Sozzani, P.; Comotti, A.; Bracco, S.; Simonutti, R. *Chem. Commun.* **2004**, 768. (e) Harada, A.; Hashidzume, A.; Takashima, Y. *Adv. Polym. Sci.* **2006**, *210*, 1. (f) Primrose, A. P.; Parves, M.; Allcock, H. R. *Macromolecules* **1997**, *30*, 670. (g) Miyata, M. In *Comprehensive Supramolecular Chemistry, Vol. 10*; Pergamon: Oxford, 1996; p 557. (h) Matsumoto, A.; Odani, T.; Sada, K.; Miyata, M.; Tashiro, K. *Nature* **2000**, *405*, 328.
- (6) (a) Uemura, T.; Kitagawa, K.; Horike, S.; Kawamura, T.; Kitagawa, S.; Mizuno, M.; Endo, K. *Chem. Commun.* **2005**, 5968. (b) Uemura, T.; Horike, S.; Kitagawa, S. *Chem. Asian J.* **2006**, *1*, 36. (c) Uemura, T.; Hiramatsu, D.; Kubota, Y.; Takata, M.; Kitagawa, S. *Angew. Chem., Int. Ed.* **2007**, *46*, 4987. (d) Uemura, T.; Ono, Y.; Kitagawa, K.; Kitagawa, S. *Macromolecules* **2008**, *41*, 87.

- (7) (a) Mattice, W. L.; Suter, U. W. *Conformation Theory of Large Molecules*; Wiley-Interscience: New York, 1994. (b) Athawale, M. V.; Goel, G.; Ghosh, T.; Truskett, T. M.; Garde, S. *Proc. Natl. Acad. Sci. U.S.A.* **2007**, *104*, 733. (c) Collison, C. J.; Rothberg, L. J.; Tree-maneeekarn, V.; Li, Y. *Macromolecules* **2001**, *34*, 2346. (d) Wachowicz, M.; White, J. L. *Macromolecules* **2007**, *40*, 5433.

**Scheme 1.** Schematic Illustration for Confinement of Single Polystyrene (PSt) Chain in the Nanochannel of **1**

$^{13}\text{C}$  CPMAS experiments were performed using a recycle delay of 6 s and a contact time of 4 ms with a spinning speed of 15 kHz. A phase-modulated Lee–Goldburg (PMLG)<sup>8</sup> heteronuclear  $^1\text{H}$ – $^{13}\text{C}$  correlation (HETCOR) experiment coupled with fast magic angle spinning (MAS) allows the registration of 2D spectra with high resolution in both the proton and carbon dimension. Phase-modulated Lee–Goldburg (PMLG)  $^1\text{H}$ – $^{13}\text{C}$  HETCOR spectra were run with an LG period of 18.9  $\mu\text{s}$ . Quadrature detection in  $t_1$  was achieved by a time proportional phase increments method. Carbon signals were acquired during  $t_2$  under proton decoupling applying a two-pulse phase modulation scheme (TPPM).<sup>9</sup>

**Solid-State  $^2\text{H}$  NMR.** The  $^2\text{H}$  NMR spectra were measured by a Varian Chemagnetics CMX-300 spectrometer at 45.8 MHz with a quadrupole echo sequence  $(\pi/2)_x - \tau - (\pi/2)_y - \tau - \text{acq}$ .  $\pi/2$  Pulse width and  $\tau$  were 2.0 and 20  $\mu\text{s}$ , respectively.  $^2\text{H}$  NMR  $T_1$  was measured by the inversion–recovery method, and the magnetization recovery was observed by using the integrated intensity of the spectrum. The simulated spectra were obtained by using the handmade program written by FORTRAN.

**$\text{N}_2$  Adsorption Measurement.** The adsorption isotherms of nitrogen at 77 K were measured with BELSORP18 volumetric adsorption equipment from Bel Japan, Inc. Nitrogen gas of high purity (99.9999%) was used. Prior to the adsorption measurements, **1** and **1**⊃PSt were treated under reduced pressure ( $<10^{-2}$  Pa) at 403 K for 5 h.

**Molecular Dynamics (MD) Simulation.** Assuming the framework structure of **1** is fixed, several equilibrium MD simulations under the NVT condition (300 K) were performed with an integration time step of 1.0 fs for PSt oligomers (tetramer and nonamer) using the universal force field (UFF)<sup>10</sup> with every 0.2 ps charge-equilibration.<sup>11</sup>

**Other Measurements.** XRPD data were collected on a Rigaku RINT 2000 Ultima diffractometer with Cu K $\alpha$  radiation. Scanning electron microscope (SEM) measurement was performed by use of a Hitachi S-3000N at an accelerating voltage of 5 kV. Differential scanning calorimetry (DSC) was carried out with a Mettler Toledo DSC822e/200.  $^{13}\text{C}$  NMR spectra were obtained with a JEOL A-500 spectrometer operated at 500 MHz. For determination of molecular weights of PSt samples, GPC was carried out at 50  $^\circ\text{C}$  on a TOSOH 8020 (TSK-gel  $\alpha$ -4000 column) with DMF as an eluent after calibration with PSt standards.

## Results and Discussion

The nanocomposite adduct of a PCP matrix with PSt (**1**⊃PSt) was obtained by radical polymerization of St included in the

host nanochannels. We used a host compound **1** with one-dimensional  $7.5 \times 7.5 \text{ \AA}^2$  nanochannels oriented along the  $c$ -axis, as depicted in Scheme 1.<sup>6a,d</sup> Scanning electron micrographs (SEM) of **1** and **1**⊃PSt showed that the crystal size and morphology of the host compound did not change during the preparation process (Figure 1). No deposition of the polymeric compound on the crystal surfaces was observed in the SEM picture of **1**⊃PSt, suggesting that the PSt chains are fully accommodated in the channels of **1**.

The glass transition temperature ( $T_g$ ), at which a drastic change in polymer motion and rotation occurs, is a typical feature of bulk polymers. Differential scanning calorimetry (DSC) of bulk PSt ( $M_n = 50\,000$ ) showed a  $T_g$  at 105  $^\circ\text{C}$  (Figure 2). In contrast, the PSt in the channels of **1** ( $M_n = 56\,000$ ) did not show such a transition. The suppression of the  $T_g$  suggests that the chain assembly of PSt was considerably changed in the host–guest adduct, as is reported in the literature for organic polymers encapsulated in nanospaces.<sup>3d,12</sup>

The framework of **1** has small apertures (ca. 4  $\text{\AA}$ ) that are large enough for the passage of small gas molecules, such as nitrogen, along the  $a$ - and  $b$ -axes through the nanochannel

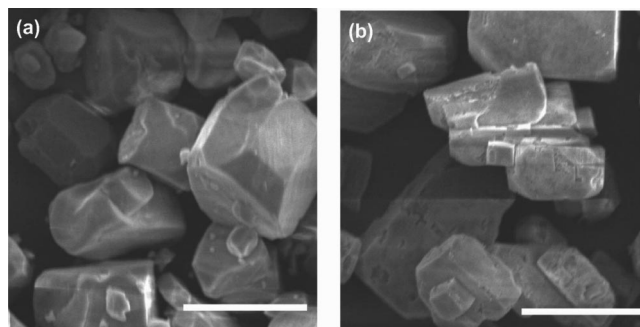


**Figure 1.** SEM images of (a) **1** and (b) **1**⊃PSt. Scale bars indicate 10  $\mu\text{m}$ .

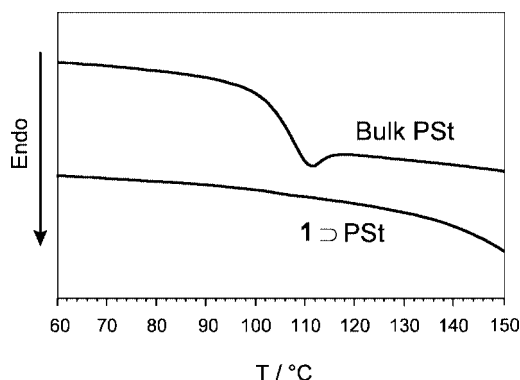


**Figure 2.** DSC profiles of bulk PSt and **1**⊃PSt.

(8) Van Rossum, B.-J.; Förster, H.; de Groot, H. J. M. *J. Magn. Reson.* **1997**, *124*, 516.

(9) Bennet, A. E.; Rienstra, C. M.; Auger, M.; Lakshmi, K. V.; Griffin, K. V. *J. Chem. Phys.* **1995**, *103*, 6951.

(10) (a) Rappé, A. K.; Casewit, C. J.; Colwell, K. S.; Goddard, W. A., III.; Skiff, W. M. *J. Am. Chem. Soc.* **1992**, *114*, 10024. (b) Casewit, C. J.; Colwell, K. S.; Rappé, A. K. *J. Am. Chem. Soc.* **1992**, *114*, 10035. (c) Casewit, C. J.; Colwell, K. S.; Rappé, A. K. *J. Am. Chem. Soc.* **1992**, *114*, 10046.

(11) Rappé, A. K.; Goddard, W. A., III. *J. Phys. Chem.* **1991**, *95*, 3358.

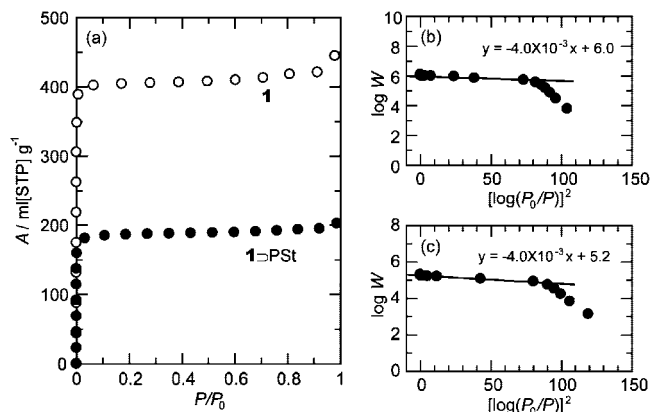


**Figure 3.** (a) Nitrogen adsorption isotherms at 77 K for guest-free **1** and **1**⊃PSt. Dubinin–Radushkevich (DR) plot of  $\text{N}_2$  adsorption data for (b) **1** and (c) **1**⊃PSt at 77 K. The loading level of PSt in **1** (weight of PSt/weight of **1**) is 0.23 in **1**⊃PSt.

**Table 1.** Micropore Parameters of **1** and **1**⊃PSt by  $\text{N}_2$  Adsorption from DR Analysis

	$W_0$ [ $\text{cm}^3(\text{STP}) \text{ g}^{-1}$ ]	$V_n$ [ $\text{cm}^3 \text{ g}^{-1}$ ]	$\beta E_0$ [ $\text{kJ mol}^{-1}$ ]
<b>1</b>	412	0.637	10.1
<b>1</b> ⊃PSt	189	0.292	10.2

walls.<sup>13</sup> Thus, nitrogen adsorption measurements at 77 K were carried out to determine the occupancy of the PSt chains in the channels of **1**. A Langmuir type I adsorption isotherm of **1** demonstrated the microporosity of the material (Figure 3a). The adsorption isotherm of  $\text{N}_2$  for **1**⊃PSt showed a decrease in the amount of adsorption compared with that of **1**, which indicates the presence of PSt chains in the nanochannels. The Dubinin–Radushkevich (DR) equation was used to characterize the detailed porous properties of **1** and **1**⊃PSt.<sup>14</sup> The DR equation is given by

$$\ln W = \ln W_0 + (A/\beta E_0)^2 \quad (1)$$

where  $W$  and  $W_0$  are the amounts of nitrogen adsorption at a relative pressure ( $P/P_0$ ) and the saturated amount of adsorption, respectively,  $E_0$  is a characteristic adsorption energy, and the parameter  $A$  is Polanyi's adsorption potential, defined as  $A = RT \ln(P_0/P)$ . The parameter  $\beta$  is the affinity coefficient and is related to the adsorbate–adsorbent interaction. The DR plots showed a linear relationship in the lower  $P_0/P$  region (Figure 3b and c), from which the micropore volume and the value of  $\beta E_0$  were obtained (Table 1). The micropore volume,  $V_m$ , was calculated from the value of  $W_0$  and the density of liquid nitrogen at 77 K ( $0.807 \text{ g cm}^{-3}$ ). The difference in pore volume corresponds to the volume occupied by PSt and is inaccessible to  $\text{N}_2$  (molecular size of  $\text{N}_2 = \text{ca. } 3.5 \text{ \AA}$ ). Considering the amount of PSt incorporated in **1**, we estimated the PSt residing in the channels to have a density of  $0.55 \text{ g cm}^{-3}$ .<sup>15</sup> Interestingly, this estimated density of a single PSt chain in **1** is considerably

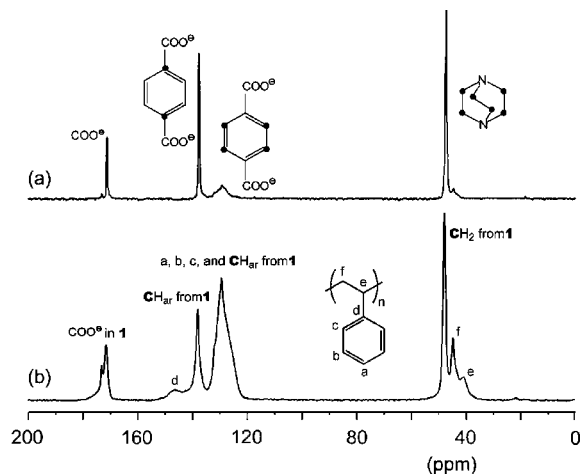


**Figure 4.**  $^{13}\text{C}$  Ramped-CP MAS NMR spectra, recorded with a spinning speed of 15 kHz and a contact time of 4 ms: (a) **1** and (b) **1**⊃PSt.

lower than that of the bulk PSt ( $1.04\text{--}1.12 \text{ g cm}^{-3}$ ),<sup>16</sup> suggesting that the polymer chains experience a larger space in the nanochannels than in the bulk.

$^{13}\text{C}$  ramped-CP MAS NMR spectra of **1** and **1**⊃PSt are compared in Figure 4. In the spectrum of the pure PCP host **1**, it is possible to recognize the resonances associated with the diamine ( $\delta_{\text{C}} = 47.7 \text{ ppm}$ ) and dicarboxylate ( $\delta_{\text{C}} = 129.0, 137.9$  and  $173.0 \text{ ppm}$ ) building blocks that comprise the metal–organic framework. In the adduct **1**⊃PSt, additional signals in both the aromatic region (about  $\delta_{\text{C}} = 129$  and  $146 \text{ ppm}$ ) and the aliphatic region ( $\delta_{\text{C}} = 44.5$  and  $40.7 \text{ ppm}$ ) are detected, because of the presence of the PSt. The signals assignments are given in Figure 4 according to the literatures.<sup>17</sup> The absence of the monomeric St residues is apparent.

Advanced 2D heteronuclear  $^1\text{H}$ – $^{13}\text{C}$  correlated (HETCOR) experiments with Lee–Goldburg homonuclear decoupling, providing high resolution in the hydrogen domain, gave a direct demonstration of the host structure of **1** and nanocomposite formation of **1**⊃PSt, as well as the intimacy between the PSt and the pore surfaces of the host. From these experiments, the connectivities between the host building blocks as well as the molecular proximity of the host vs guest moieties were unambiguously established by measuring and correlating the heteronuclear  $^1\text{H}$ – $^{13}\text{C}$  dipole–dipole interactions. The 2D spectrum of the empty host **1** (Figure 5a), at the short contact time of 1 ms, clearly shows the correlations between the hydrogens and carbon atoms in close proximity within the same building block. Instead, at longer contact times (Figure 5b), the correlations between the bdc and ted building blocks is clearly highlighted by the cross-signal  $\delta_{\text{H}} = 7.6 \text{ ppm}$ ,  $\delta_{\text{C}} = 47.7 \text{ ppm}$ , which shows that the aromatic hydrogens of the terephthalic group can transfer the magnetization to the carbon of the diamine group (blue area). In the 2D spectrum of **1**⊃PSt, at a 1 ms contact time, we observed separately the correlation peaks of the aliphatic hydrogens of the PSt ( $\delta_{\text{H}} = 1 \text{ ppm}$ ) with their covalently bonded carbons; the aliphatic hydrogens of the

(12) (a) Moller, K.; Bein, T.; Fischer, R. X. *Chem. Mater.* **1998**, *10*, 1841. (b) Ji, X.; Hampsey, J. E.; Hu, Q.; He, J.; Yang, Z.; Lu, Y. *Chem. Mater.* **2003**, *15*, 3656.  
 (13) Dybtsev, D. N.; Chun, H.; Kim, K. *Angew. Chem., Int. Ed.* **2004**, *43*, 5033.  
 (14) Dubinin, M. M. *Chem. Rev.* **1960**, *60*, 235.  
 (15) Pereira, C.; Kokotailo, G. T.; Gorte, R. J. *J. Phys. Chem.* **1991**, *95*, 705.

(16) *Polymer Handbook*, 2nd ed.; Brandrup, J., Immergut, E. H., Eds; John Wiley & Sons: New York, 1975.  
 (17) (a) Ebdon, J. R.; Huckerby, T. N. *Polymer* **1976**, *17*, 170. (b) Schaefer, J.; Sefcik, M. D.; Stejskal, E. O.; McKay, R. A.; Dixon, W. T.; Cais, R. E. *Macromolecules* **1984**, *17*, 1107. (c) Miyoshi, T.; Tagakoshi, K.; Terao, T. *Macromolecules* **1997**, *30*, 6582. (d) Duna, M. G.; Novak, B. M.; Schmidt-Rohr, K. *Solid State Nucl. Magn. Reson.* **1998**, *12*, 119.

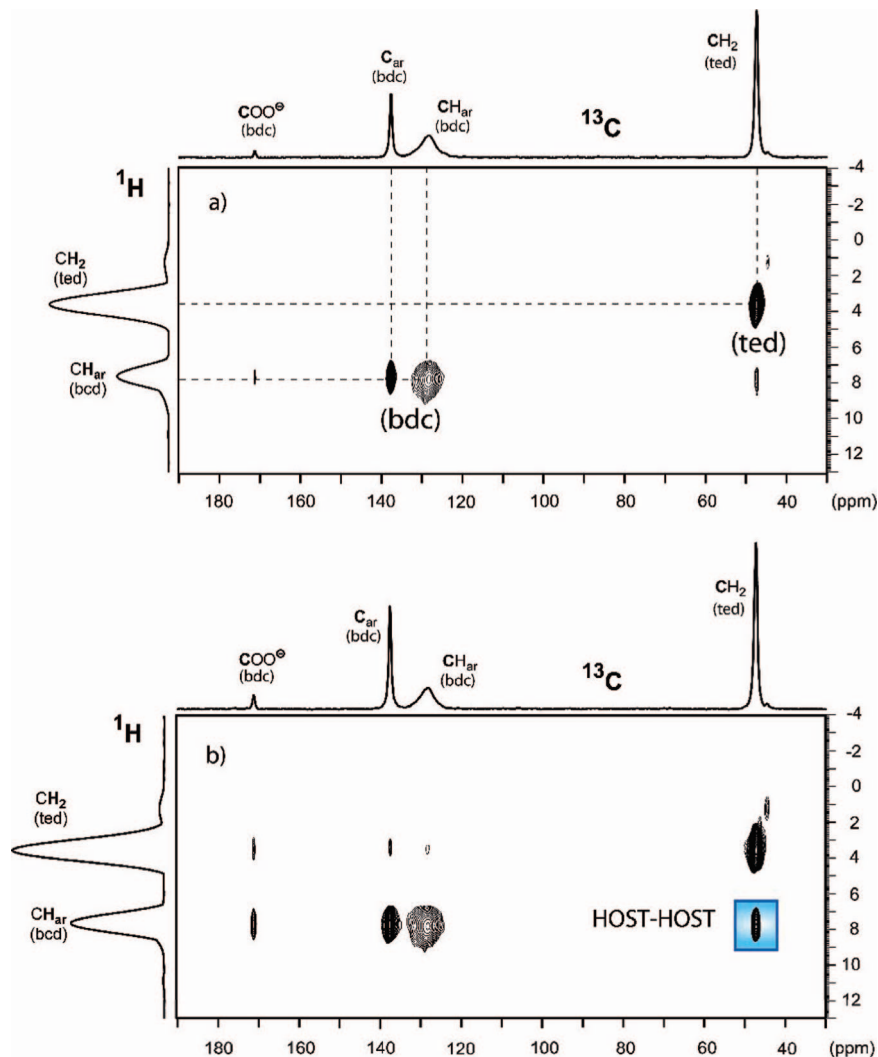


**Figure 5.** Fast magic angle spinning 2D heterocorrelated NMR spectra, with Lee–Goldburg homonuclear decoupling, of the empty host **1**: contact times of (a) 1 ms and (b) 5 ms were used. A spinning speed of 15 kHz was applied. In the short contact time experiments only intramolecular correlations of protons to vicinal carbons are essentially present. Longer cross-polarization time resulted in new correlation peaks that pertain to through space intermolecular interactions between bdc and ted in the host structure of **1**.

polymer also show through-space relationships with the  $\text{CH}_{\text{ar}}$  aromatic carbons of PSt (Figure 6a, highlighted in blue color). The correlation signal between the aliphatic hydrogens and the  $\text{C}_{\text{d}}$  aromatic carbons of PSt, shown as a low intensity signal at 146 ppm in the 1D  $^{13}\text{C}$  spectrum (Figure 4), is not observed due to its negligible intensity. The 2D NMR spectrum, at a contact time of 5 ms, shows the intermolecular correlations of the hydrogen atoms in the main chain of PSt with the carboxylate groups and the aromatic rings of the bdc unit, as well as with the carbon atoms of the ted building blocks of the host matrix (Figure 6b, orange area). In turn, the hydrogen atoms of the ted unit ( $\delta_{\text{H}} = 3.6$  ppm) correlate with the carbon atoms in the main chain of PSt. Thus we have demonstrated, for the first time, the formation of extended, hybrid metal–organic/organic interfaces fabricated between a PCP matrix and an organic polymer.

In amorphous bulk polymer systems, the molecular dynamics of polymer chains are strongly associated with the heterogeneous interpolymer and intrapolymer interactions.<sup>18</sup> In the case of

polymers containing side chains, cooperative motions of the main chains and side chains also affect the overall polymer properties, which results in many difficulties associated with analyzing the nature of polymer motions. The formation of single polymer chains confined in regular one-dimensional nanochannels will afford unique molecular dynamics that are different from those observed in the bulk state. However, analysis of single PSt homopolymer chains confined in nano-spaces has not yet been reported.

In this work, we prepared a bulk  $[\text{D}_5]\text{PSt}$  sample with selective deuteration of the phenyl rings and a nanocomposite of  $[\text{D}_5]\text{PSt}$  with **1** ( $[\text{D}_5]\text{PSt}$ ) for solid-state  $^2\text{H}$  NMR measurements.<sup>19</sup> The solid-state  $^2\text{H}$  NMR technique is effective for studying the environment and motion of polymeric materials.<sup>20</sup> The  $^2\text{H}$  NMR spectrum of bulk  $[\text{D}_5]\text{PSt}$  (Figure 7) shows a major splitting of the singularities of  $\pm 62.5$  kHz and a minor splitting of  $\pm 20$  kHz. These spectra are consistent with those presented in the literatures.<sup>17b,20,21</sup> We tried to theoretically

(18) (a) Barbara, P. F.; Gesquiere, A. J.; Park, S.-O.; Lee, Y. J. *Acc. Chem. Res.* **2005**, *38*, 602. (b) Spiess, H. W. *Chem. Rev.* **1991**, *91*, 1321.

(19) We have also measured  $^2\text{H}$  NMR of a nanocomposite of **1** and  $[\text{D}_2]\text{PSt}$  (main chain deuteration); however, the quality of the obtained spectra was not enough for detailed analysis.

(20) Spiess, H. W. *Colloid Polym. Sci.* **1983**, *261*, 193.

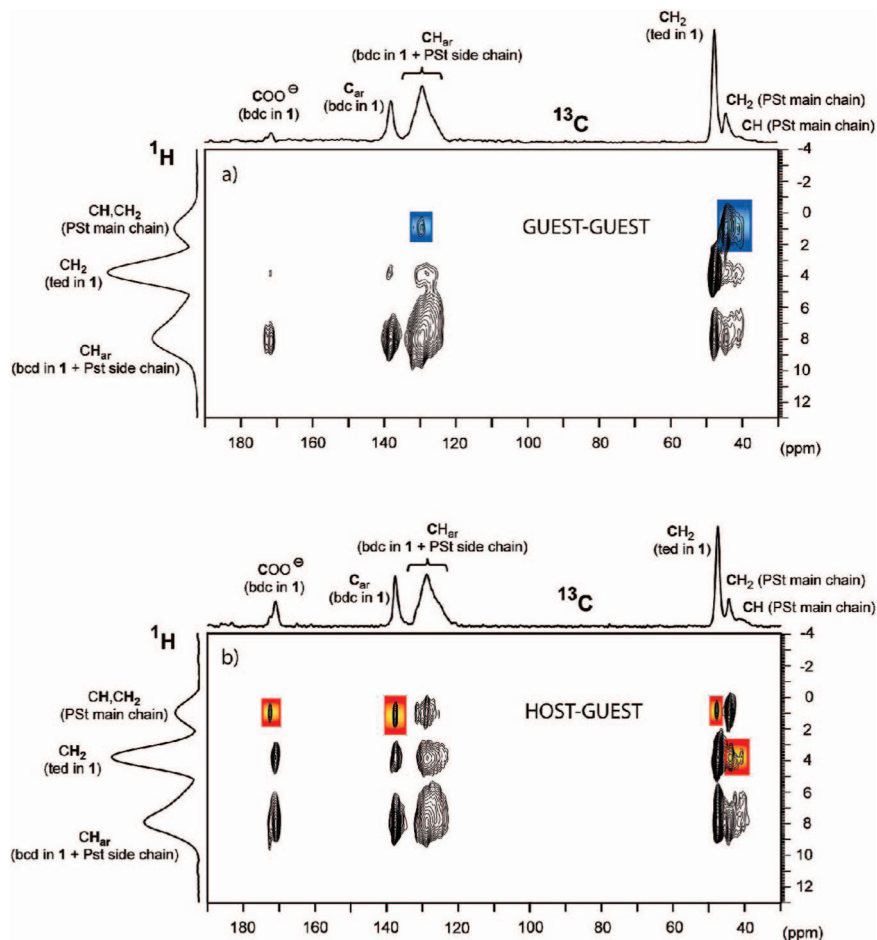


**Figure 6.** Fast magic angle spinning 2D heterocorrelated NMR spectra, with Lee–Goldburg homonuclear decoupling, of  $1D_5$ Pst: contact times of (a) 1 ms and (b) 5 ms were used. A spinning speed of 15 kHz was applied.

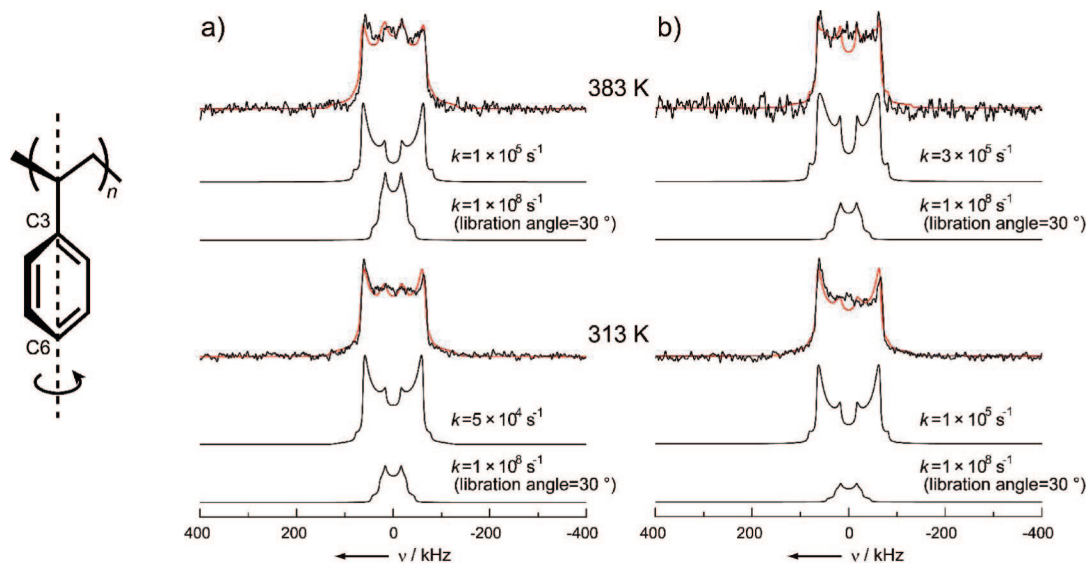


**Figure 7.** Selected  $^2\text{H}$  NMR spectra of (a) bulk  $[D_5]$ PSt and (b)  $1D_5$ PSt (black, observed; red, simulated) at 313 and 383 K. The two spectra below observed spectra represent the simulated components ( $\pi$ -flipping and librational motions). The red lines are sum of both simulated subspectra.

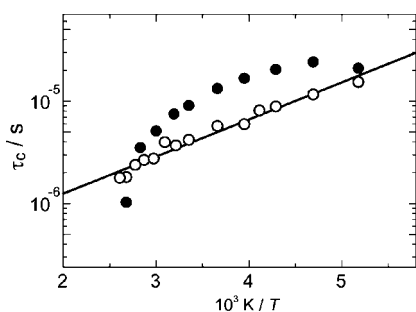
reproduce the obtained spectra by assuming the coexistence of two contributions from the phenyl groups, performing relatively slow and fast flipping motions. Consequently, we succeeded in obtaining a good line-shape fitting by employing the system with a dominant low-frequency ( $k_1$ :  $\sim 10^5 \text{ s}^{-1}$ )  $180^\circ$  flip of the

phenyl rings around the C3–C6 axis, together with rapid phenyl rotation ( $k_2$ :  $\sim 10^8 \text{ s}^{-1}$ ) with librational motion ( $k_3 = 10^{10} \text{ s}^{-1}$ ), as shown in Table 2. From these motional simulations, only 6% of the phenyl rings in PSt participate in the wobbling rotation at 313 K, and the content of the mobile phenyl rings, presenting

**Table 2.** Fit Parameters for the  $^2\text{H}$  NMR Spectra of Bulk  $[\text{D}_5]\text{PSt}$  and  $1\text{D}[\text{D}_5]\text{PSt}$  at 383 and 313 K<sup>a</sup>

	bulk $[\text{D}_5]\text{PSt}$ at 383 K	bulk $[\text{D}_5]\text{PSt}$ at 313 K
$k_1$ ( $\text{s}^{-1}$ )	$1 \times 10^5$ (89%)	$5 \times 10^4$ (94%)
$k_2$ and $k_3$ ( $\text{s}^{-1}$ )	$k_2 = 1 \times 10^8$	$k_2 = 1 \times 10^8$
with librational	$k_3 = 1 \times 10^{10}$	$k_3 = 1 \times 10^{10}$
angle (deg)	( $\pm 30^\circ$ ) (11%)	( $\pm 30^\circ$ ) (6%)
	$1\text{D}[\text{D}_5]\text{PSt}$ at 383 K	$1\text{D}[\text{D}_5]\text{PSt}$ at 313 K
$k_1$ ( $\text{s}^{-1}$ )	$3 \times 10^5$ (94%)	$1 \times 10^5$ (97%)
$k_2$ and $k_3$ ( $\text{s}^{-1}$ )	$k_2 = 1 \times 10^8$	$k_2 = 1 \times 10^8$
with librational	$k_3 = 1 \times 10^{10}$	$k_3 = 1 \times 10^{10}$
angle (deg)	( $\pm 30^\circ$ ) (6%)	( $\pm 30^\circ$ ) (3%)

<sup>a</sup> Rate of slow phenyl flip ( $k_1$ ) and rate of fast phenyl rotation ( $k_2$ ) with librational motion rate ( $k_3$ ) are listed. The relative intensity (%) of each fraction is also included in the table.

**Figure 8.** Correlation times  $\tau_c$  of bulk  $[\text{D}_5]\text{PSt}$  (●) and  $1\text{D}[\text{D}_5]\text{PSt}$  (○) as a function of temperature.

rotational and librational motion, reaches 11% at 383 K.<sup>17b,20,21</sup> The NMR patterns of  $1\text{D}[\text{D}_5]\text{PSt}$  reveal that the component associated with the singularities and resulting from the  $180^\circ$  flip of the phenyl rings was increased (97% at 313 K) (Table 2), when compared with those in the spectrum of bulk  $[\text{D}_5]\text{PSt}$ .

In order to elucidate the detailed dynamics of the single PSt chains in the channels, we focused on the dominant phenyl flip motion and measured its spin–lattice relaxation time ( $T_1$ ) in the temperature range from 193 to 393 K. The variable temperature  $T_1$  measurement can provide information about the range of motional frequency and motional heterogeneity. More specifically, the  $T_1$  measurements of  $^2\text{H}$  nuclei of deuterated compounds enable us to understand the partial dynamics of the target molecule. The temperature dependence of  $T_1$  showed the correlation time ( $\tau_c$ ) for the  $180^\circ$  flip of the phenylene ring, and Figure 8 displays the temperature dependence of  $\tau_c$  for bulk  $[\text{D}_5]\text{PSt}$  and  $1\text{D}[\text{D}_5]\text{PSt}$ . Assuming the asymmetry parameter of  $\eta = 0$  in both systems,  $T_1$  can be written as follows:<sup>22</sup>

$$\frac{1}{T_1} = \frac{1}{5} \left( \frac{\omega_Q}{\omega_0} \right)^2 \frac{1}{\tau_c} \sin^2(2\beta) \quad (2)$$

$$\omega_Q = \frac{3e^2Qq}{4\hbar}$$

where  $\omega_0$ ,  $e^2Qq/\hbar$ , and  $\beta$  denote the angular frequency and the Larmor frequency of the  $^2\text{H}$  nucleus, the quadrupole coupling

constant, and the angle between the jump axis and the principal axis of the electric field gradient tensor at the  $^2\text{H}$  nucleus, respectively. Assuming an Arrhenius-type relationship,  $\tau_c$  is given by

$$\tau_c = \tau_{c0} \exp\left(\frac{E_a}{RT}\right) \quad (3)$$

where  $\tau_{c0}$  and  $E_a$  are the correlation time at infinite temperature and the activation energy for the  $180^\circ$  flip of the phenylene ring of PSt, respectively. In Figure 8, the mean  $\tau_c$  for bulk  $[\text{D}_5]\text{PSt}$  provides a nonlinear profile in log scale, especially in the high temperature region (near to  $T_g$ ). This is the result of multiple phenyl flippings, showing a broad distribution of  $\tau_c$  from milliseconds to microseconds.<sup>21b</sup> Such a wide motional distribution originates from the heterogeneous local environment of the phenyl rings in bulk PSt.<sup>21b</sup> Because of this wide motional distribution, it is impossible to determine the activation energy ( $E_a$ ) of the  $180^\circ$  phenyl flip motion of bulk PSt over this entire temperature region. In fact, the  $E_a$  values obtained in previous NMR, dielectric, and theoretical studies were not solid, showing a wide range of values from 38 to 420  $\text{kJ mol}^{-1}$ .<sup>17b,21,23</sup> In contrast to the bulk PSt system, the profile of the mean  $\tau_c$  for  $1\text{D}[\text{D}_5]\text{PSt}$  was linear over the entire temperature range studied, which clearly suggests that PSt in **1** represents a quasi-single-type phenyl flipping motion in this temperature region. This increased uniformity of motion can lead to the successful estimation of  $E_a$  for the phenyl flip of the single PSt chain confined in the nanochannels ( $E_a = 8.8 \text{ kJ mol}^{-1}$ ), where the calculated  $E_a$  value for the phenyl flip of the single PSt chain is considerably low. This unusually small energy barrier can be ascribed to the large volume available to the PSt chains in the nanochannels of **1**.<sup>21b</sup> The less steric hindrance of the phenyl rings of the single PSt chain in **1** would contribute to the low  $E_a$  value of the phenyl rings.

The chain conformations of PSt oligomers in the channel of **1**, simulated using the molecular dynamics (MD) method, agree with the unique molecular motion observed in the NMR measurements. In the MD simulation, the conformation of the PSt tetramer is far from linear in the nanochannel: it represents the formation of chain bending resulting from face-to-face interactions between the terminal St moieties and the pore walls of **1** (Figure 9a). However, the MD simulation of the PSt nonamer in **1** shows a linear single-chain structure of PSt in the middle part (Figure 9b), even though the benzene units of the oligomer end groups still interact with the pore walls. These results clearly suggest that the introduction of a higher molecular weight PSt into the channels of **1** will lead to a highly extended linear conformation of the single PSt chain, which contrasts significantly with the random chain-entangled structures that essentially occur in the bulk state. Thus, the unprecedented homogeneous mobility of the phenyl rings of PSt with low  $E_a$  could be ascribed to the successful formation of single PSt chains confined in the flat and smooth one-dimensional nanochannels of the crystalline host **1**.

## Conclusions

The inclusion polymerization of St in a PCP architecture led to the fabrication of an innovative metal–organic nanocomposite

(21) (a) Spiess, H. W. *J. Mol. Struct.* **1983**, *111*, 119. (b) Kulik, A. S.; Prins, K. O. *Polymer* **1993**, *34*, 4635.  
(22) (a) Hiyama, Y.; Silvertown, J. V.; Torchia, D. A.; Gerig, J. T.; Hammond, S. J. *J. Am. Chem. Soc.* **1986**, *108*, 2715. (b) Mizuno, M.; Hamada, Y.; Kitahara, T.; Suhara, M. *J. Phys. Chem. A* **1999**, *103*, 4981.

(23) (a) Yano, O.; Wada, Y. *J. Polym. Sci. Polym. Phys. Ed.* **1971**, *9*, 669. (b) Tonelli, A. E. *Macromolecules* **1973**, *6*, 682. (c) Tanabe, Y. *J. Polym. Sci., Polym. Phys. Ed.* **1985**, *23*, 601. (d) Khare, R.; Paulaitis, M. E. *Macromolecules* **1995**, *28*, 4495.

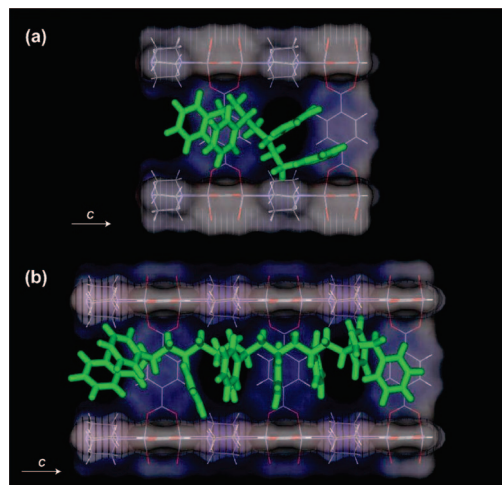


**Figure 9.** Typical MD structures (ending snapshots) of (a) PSt tetramer and (b) nonamer encapsulated in the nanochannel of **1**. Stereoregularities of the model oligomers are similar to that of the real PSt.

material containing single PSt chains confined in the nanochannels. The application of advanced solid-state NMR techniques enabled the detection of extended metal–organic/organic hybrid interfaces between the crystalline walls and the polymer confined in the framework. 2D NMR experiments exploiting hydrogen and carbon nuclei and homonuclear Lee–Goldburg decoupling revealed, for the first time, the topology of the polymer residing

within the PCP matrix as well as the close spatial interactions between the guest PSt occupying the nanochannels and the host. Conformational studies and chain dynamics from  $^2\text{H}$  NMR and molecular simulations support the unprecedented behavior of the PSt chain, namely homogeneous side-chain mobility and considerably low activation energy. This behavior originates from both the linear extension of the single-chain conformation in a regular environment and the exclusion of the multiple interactions observed in the bulk material. We believe that our results will contribute to the evolution of new systems providing significant insights into the polymer confinement effects as well as inherent properties of single polymer chains, because PCPs can afford tailor-made nanoporous materials that exhibit the properties of both the reaction vessel for the monomers and the isolation/confinement of the resultant polymer.

**Acknowledgment.** This work was supported by PRESTO-JST, a Grant-in-Aid for Scientific Research in a Priority Area “Chemistry of Coordination Space” (#434), and a Grant-in-Aid for Young Scientists (B) (#17750125) from the Ministry of Education, Culture, Sports, Science and Technology, Government of Japan.

**Supporting Information Available:** Solid-state  $^1\text{H}$  MAS spectra and stereostuctures of PSt oligomers employed in MD simulation. This material is available free of charge via the Internet at <http://pubs.acs.org>.

JA800087S